Materials Advances

REVIEW

View Article Online
View Journal | View Issue

Cite this: *Mater. Adv.*, 2024, 5, 3082

Enlisting electrochemistry to reveal melanin's redox-related properties

Eunkyoung Kim,[ab] Zheng Wang,[c] Jun Wei Phua,[d] William E. Bentley,[abe] Ekaterina Dadachova,[f] Alessandra Napolitano[g] and Gregory F. Payne *[ab]

Received 21st December 2023,
Accepted 5th March 2024

DOI: 10.1039/d3ma01161e

rsc.li/materials-advances

Melanin has been surprisingly difficult to characterize using either bottom-up studies focused on molecular structure or top-down studies focused on functional properties. We have been developing electrochemical methods to understand the redox-activities of melanin. These studies show that melanins from various sources: (i) are reversibly redox-active; (ii) have redox potentials in the mid-physiological range; and (iii) react with a broad range of electron-donors (*i.e.*, reductants) and acceptors (*i.e.*, oxidants). Spectroelectrochemically-based operando methods have shown that when melanin is exchanging electrons, it also undergoes changes in its redox state. The observation that melanin can exist in two (or possibly more) oxidized or reduced states helps to explain some of its context-dependent behaviors. For instance, when melanin is in a reduced state, it has donate-able electrons that can quench an oxidative radical or partially-reduce O_2 to generate reactive oxygen species (ROS). Further, melanin can promote redox-cycling when it is located in metabolically-active contexts that are characterized by steep O_2-gradients because short diffusion distances separate aerobic from anaerobic conditions. We suggest that future studies may enable a fuller understanding of how melanin's redox activities contribute to its observed electrical conductivities (ionic and/or electrical), and if melanin's redox-capacitor properties confer a biological benefit (*e.g.*, for energy harvesting).

Introduction

Melanins are a broad class of aromatic macromolecules that are ubiquitous in nature but have proven difficult to characterize.[1–4] Bottom-up studies[1,2,4–10] aimed at revealing molecular structure indicate that unlike other biomacromolecules (*e.g.*, proteins and nucleic acids), melanins do not have a common monomeric unit or linkage, and do not have a characteristic sequence, size, or architecture (linear *vs.* branched). In fact, there is still debate whether melanin is a high molecular weight polymer or an aggregate of lower molecular weight oligomers.[7–9] Top-down studies of melanin's functional properties, rather than providing clarity, have often shown dichotomies. For instance, melanin's broad band optical absorption rather than clarifying structure–function relationships suggested a chemical disorder model,[9–13] while melanin's optical properties can have either beneficial (*e.g.*, photoprotection)[14–17] or detrimental (*e.g.*, photosensitizing) effects.[18,19] Melanin's electrical properties have attracted considerable attention with results spurring debates of the nature of this electrical conductivity (ionic *vs.* electronic).[12,20–26] In immunity, insects are believed to generate melanins as a defense response to pathogen threats,[27,28] while pathogenic fungi are believed to synthesize melanins to counter host defenses.[29–32] And melanin's redox properties seem to be able to offer antioxidant protection[33–35] but, in some cases, induce pro-oxidant damage.[13,36–38]

Since melanin's redox properties seem especially important to its biological or technological function, there have been several attempts to investigate these redox properties.[39,40] Pulse radiolysis studies[39,40] demonstrated that melanin can act as a radical scavenger for oxidizing and reducing free radicals. Another study[41] showed that melanins can mediate the transfer of electrons from electron donors to electron acceptors. Also, several groups[42–44] are using electrochemical methods to detect the redox-related electron transfer with melanin.

Several years ago, we initiated our studies on melanin. In particular, we adapted electrochemical methods to probe

[a] *Institute for Bioscience and Biotechnology Research, University of Maryland, College Park, Maryland 20742, USA. E-mail: gpayne@umd.edu; Fax: +1-301-314-9075; Tel: +1-301-405-8389*
[b] *Robert E. Fischell Institute for Biomedical Devices, University of Maryland, College Park, Maryland 20742, USA*
[c] *Center for Bio/Molecular Science and Engineering, US Naval Research Laboratory, Washington, DC 20375, USA*
[d] *Insectta Pte. Ltd., 8 Cleantech Loop, Singapore 637145, Singapore*
[e] *Fischell Department of Bioengineering, University of Maryland, College Park, Maryland 20742, USA*
[f] *College of Pharmacy and Nutrition, University of Saskatchewan, Saskatoon, S7N 5E5, SK, Canada*
[g] *Department of Chemical Sciences, University of Naples Federico II, Via Cintia 4, I-80126 Naples, Italy*

redox-activities.[45–53] Here, we summarize how electrochemical studies are revealing important features of melanin's redox activities and how these methods help to elucidate the significance of redox-context, integral to understanding some of melanin's dichotomies. Thus, the goal of this report is to illustrate how the creative use of electrochemistry can assist in characterizing important properties of melanin.

Mediated electrochemical probing (MEP)

In initial studies,[45,52] we examined the melanin from *Sepia officinalis* (*i.e.*, cuttlefish) which is a readily available natural eumelanin of high purity. *Sepia* melanin is water-insoluble with a granular microstructure (100–200 nm) illustrated in Fig. 1a. Our mediated electrochemical probing (MEP) approach to observe redox activity is illustrated in Fig. 1b. First, the melanin is entrapped adjacent to an electrode surface within a non-conducting hydrogel film based on the aminopolysaccharide chitosan.[54] This hydrogel locally entraps the melanin but remains permeable to low molecular weight mediators (*i.e.*, electron shuttles).

Second, the electrode with the melanin-containing chitosan hydrogel is immersed in a solution containing mediators. Fig. 1b illustrates two mediators. One mediator has a relatively reducing redox potential (often we use $Ru(NH_3)_6Cl_3$, Ru^{3+}, E° = −0.25 *vs.* Ag/AgCl) and can shuttle electrons from the electrode to the melanin when reducing potentials are applied at the electrode. As illustrated, this "charging" of melanin with electrons occurs through a Ru^{3+}-based reductive redox-cycling mechanism. The second mediator has a relatively oxidizing redox potential (*e.g.*, often we use ferrocene dimethanol, Fc, E° = +0.25 V) and can "discharge" electrons from the melanin to the electrode (through an oxidative redox-cycling mechanism) when oxidizing potentials are applied at the electrode.

Third, a sequence of potential (*i.e.*, voltage) inputs is imposed at the electrode. Fig. 1c shows a cyclically oscillating potential that becomes: sufficiently negative during the reductive segment to engage the reducing mediator (Ru^{3+}) in reductive redox-cycling; and sufficiently positive during the oxidative segment to engage the oxidizing mediator (Fc) in oxidative redox-cycling.

Fourth, the output (*i.e.*, electrical current) is measured and interpreted in terms of the underlying redox-based electron transfer mechanisms. For instance, the outputs in the time-series plots of Fig. 1c show that oscillating currents for the melanin-containing chitosan film are amplified relative to those for the control melanin-free chitosan film probed with the same two mediators. Fig. 1d shows a traditional phase-plane representation of the same data: this plot more clearly shows the relationship between the observed output current

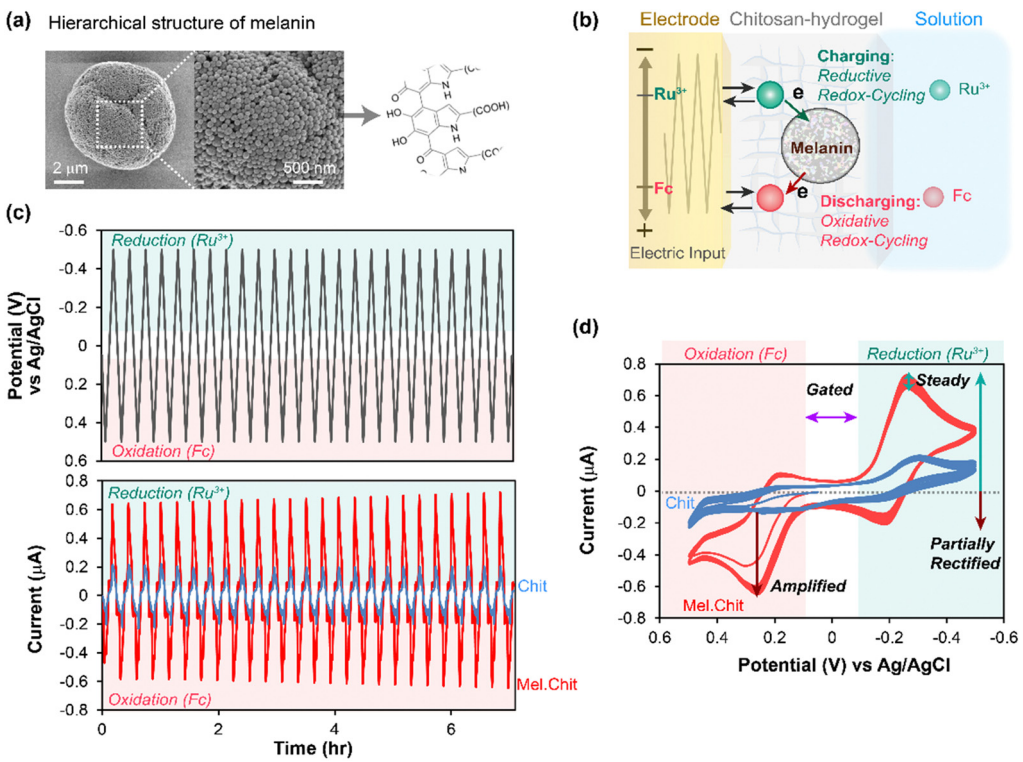

Fig. 1 Mediated electrochemical probing (MEP) with *Sepia* melanin. (a) *Sepia* melanin is water-insoluble, particulate and a model for natural eumelanin. (b) Melanins entrapped within a hydrogel film of the aminopolysaccharide chitosan are probed using mediators (*e.g.*, Ru^{3+} and Fc) and oscillating electrode-imposed potential inputs. (c) Time-series measurements show oscillating output current (*i*) responses to a cyclically-imposed potential (*E*) input. (d) Standard cyclic voltammograms (CVs) are *i*–*E* phase-plane plots that more clearly illustrate the relationship between the imposed input and observed output. [Adapted with permission from ref. 45. Copyright 2018, American Society, Washington, DC.].

response and the imposed input potential (time is not explicitly shown in this phase-plane plot). Fig. 1d illustrates several characteristic features of reversibly redox-active but non-conducting films that can accept and donate electrons through mediator-based redox-cycling mechanisms. First, the output currents are gated by the mediators: this provides evidence that the mediators are the primary mechanism for electron-flow to/from melanin. Second, the currents are also amplified (relative to a melanin-free control film) and partially rectified (the currents for each mediator are selectively amplified for either oxidation or reduction): this is consistent with the redox-cycling mechanisms being responsible for transferring electrons to and from the melanin. Third, the current response appears nearly steady (*i.e.*, time invariant): this provides evidence that the melanin can be reversibly and repeatedly oxidized and reduced.

From initial MEP studies, it was possible to conclude that *Sepia* melanin is reversibly redox-active (it can be repeatedly oxidized and reduced) and it has a redox potential in the mid-physiological region. Further, if we think of melanin as a type of redox catalyst (*i.e.*, it catalyzes the transfer of electrons from reductants to oxidants), then its ability to react with Ru^{3+} and Fc provides initial evidence that its substrate range may be broad. Using similar MEP measurements, we observed similar redox-activities for various synthetic or natural melanins, as well as other natural (*e.g.*, insoluble dietary antioxidants)[55] and synthetic catecholic materials (*e.g.*, catechol–chitosan and polydopamine).[53,56–62]

There were two important extensions of this initial MEP method. First, we compared natural and synthetic models of eumelanin and pheomelanin using three mediators with different redox potentials, and we observed that pheomelanin has a more oxidative redox-potential than eumelanin: this observation may explain pheomelanin's pro-oxidant activities.[49] Second, we performed studies in which we replaced one of the mediators with a chemical of interest and we observed that some redox-active environmental toxins (*i.e.*, paraquat)[48] and drugs (*e.g.*, clozapine or acetaminophen)[47] can undergo redox-cycling with melanin. While such *in vitro* MEP measurements cannot prove an *in vivo* activity, it has revealed a previously unknown mechanism of potential biological relevance to chemical toxicities and drug activities.[51]

In summary, MEP allows the immobilized melanin to be repeatedly and sequentially exposed to oxidative and reductive conditions (*i.e.*, potentials) while observing its redox-based electrical response (*i.e.*, the resulting currents). From the perspective of properties, these studies are revealing a deeper understanding of melanin's redox activity. From the perspective of biological function, these results illustrate that melanin may not be an inert bystander in biology but rather may actively participate in redox biology.

Spectroelectrochemical probing

Various properties are expected to be linked to melanin's redox activity, and we extended MEP to study the radical scavenging properties of two types of melanin: the eumelanin from *Sepia*, and a fungal melanin derived from 1,8-dihydroxynaphthalene (DHN).[46,63] Compared to eumelanin, fungal DHN melanin is synthesized from an entirely different precursor and pathway,[64,65] and Fig. 2a shows this DHN melanin is localized in the fungal cell wall, as illustrated by the SEM and TEM images.[46] Fungal melanin "ghosts" were prepared by treating the melanized fungal cells with strong detergent and acid.[63] This cell-wall bound DHN melanin is proposed to confer radiation-protection to the fungi. As described in the previous section, we entrapped the *Sepia* melanin and fungal melanin ghosts in chitosan hydrogels adjacent to the electrode, and we extended redox probing in two important ways.

First, we used the electrode to generate free radicals with spatiotemporal and quantitative control. Specifically, we studied two different free radicals, paraquat ($PQ^{+\bullet}$) and 2,2′-azinobis(3-ethylbenzothiazoline-6-sulfonic acid) ($ABTS^{+\bullet}$), each of which could be directly-generated electrochemically without the need for adding reagents. However, as illustrated in Fig. 2b, these two radicals are fundamentally different. The $PQ^{+\bullet}$-radical is generated by accepting an electron and its quenching requires donation of this electron (*i.e.*, $PQ^{+\bullet}$ is a reductive radical). In contrast, the $ABTS^{+\bullet}$-radical is generated by donating an electron and its quenching requires acceptance of an electron (*i.e.*, $ABTS^{+\bullet}$ is an oxidative radical). As illustrated in Fig. 2b, it is possible to perform redox probing experiments using PQ^{2+} as the reductive redox-cycling mediator and ABTS as the oxidative redox-cycling mediator. If these two mediators are used in the same experiment, and a cyclically-imposed electrode potential is imposed, then the $PQ^{+\bullet}$ and $ABTS^{+\bullet}$ radicals are generated in an oscillating manner with opposite phases (*i.e.*, the $PQ^{+\bullet}$-radical is generated during the reductive segment while the $ABTS^{+\bullet}$-radical is generated during the oxidative segment).

Secondly, we extended MEP to observe spectral output responses while monitoring electrical output responses. In general, spectroelectrochemical analysis is valuable because it enables electrical measurements of activity to be complemented by simultaneous spectral measurements which provide insights of molecular structure. Specifically, we can use spectral analysis to monitor radical generation/quenching because the $PQ^{+\bullet}$-radical has a characteristic blue color (λ_{max} = 394 nm) while the $ABTS^{+\bullet}$-radical has a characteristic green color (λ_{max} = 420 nm). Experimentally, we used a honeycomb gold electrode illustrated in Fig. 2c to perform these spectroelectrochemical measurements, and measured the optical response at 394 nm since both radicals have measurable absorbance at this wavelength. As illustrated, this electrode has holes that can serve as the optical window for spectral analysis.

Fig. 2d shows time-series input-output curves when a cyclic input potential was imposed in the presence of both PQ^{2+} and ABTS.[46] During the oxidative segment (when the imposed electrode potential is positive), the output response shows both peaks in oxidative current and absorbance at 394 nm associated with the generation $ABTS^{+\bullet}$-radical. For the control chitosan-coated electrode without melanin, a weak oxidative peak current and a strong absorbance peak are observed. The absorbance peak in this control film arises from the electrochemical-generation of the

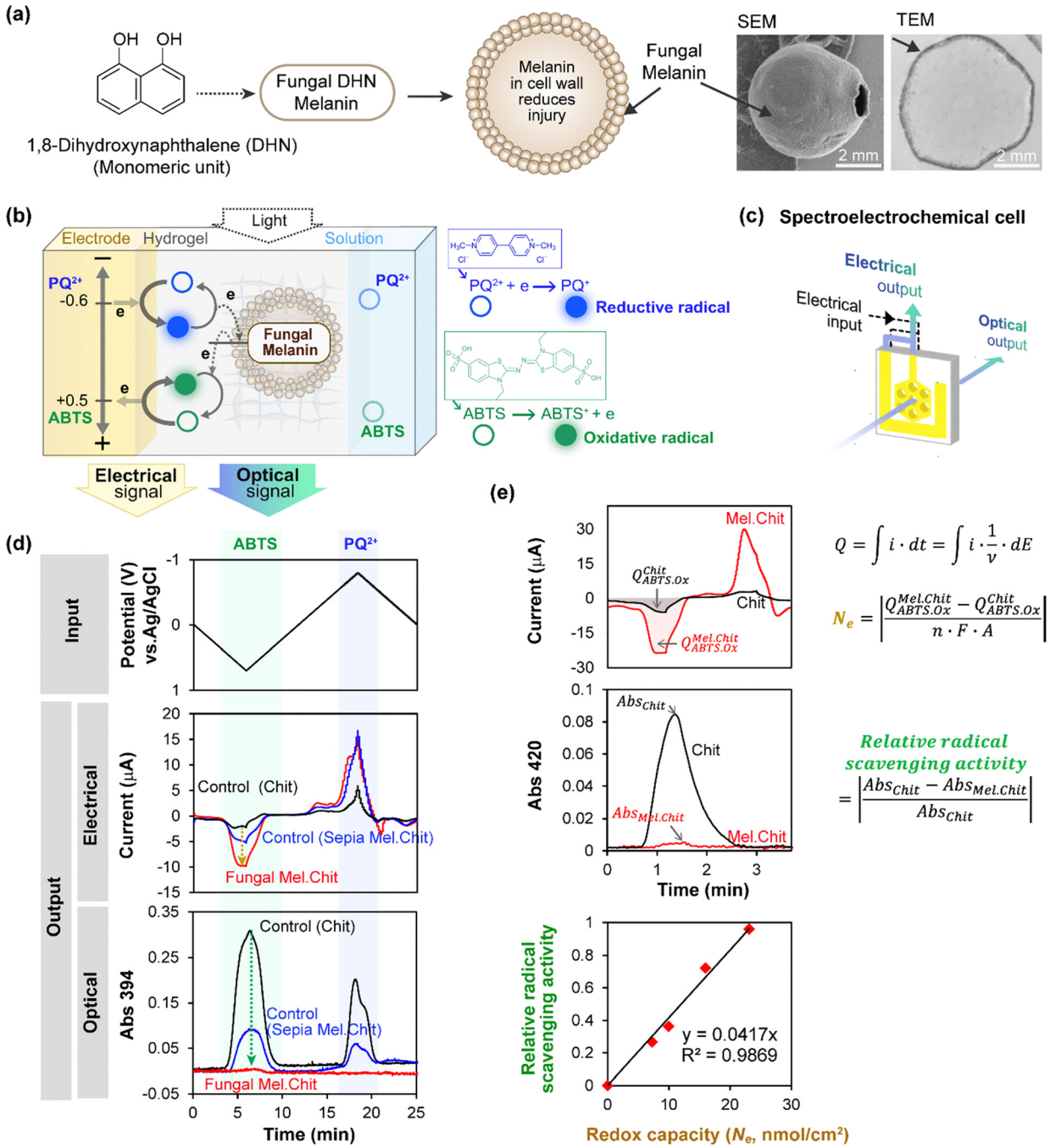

Fig. 2 Spectroelectrochemical analysis of free radical quenching by fungal 1,8-dihydroxynaphthalene (DHN) melanin. (a) This DHN melanin is localized in the fungal cell wall. (b) Fungal "ghosts" were probed using electrochemically-generated radicals derived from paraquat (reductive free radical) and ABTS (oxidative free radical). (c) A honeycomb gold electrode provides the optical window for simultaneous electrical and spectral analysis. (d) Time-series input-output curves show cyclically-imposed electrical inputs (*i.e.*, potential) induce oscillating electrical and spectral output responses (*i.e.*, current and absorbance). (e) Semi-quantitative analysis shows a linear correlation between melanin's radical-scavenging and redox activities. [Adapted with permission from ref. 46. Copyright 2017, American Society, Washington, DC.].

$ABTS^{+\bullet}$-radical when oxidative potentials are imposed, and subsequently the $ABTS^{+\bullet}$-radical is electrochemically-reduced (*i.e.*, quenched) when the electrode potential is cycled to more reductive values. When either *Sepia* or fungal DHN melanin is included in the hydrogel film, the oxidative peak currents are amplified while the absorbance peaks in the oxidative segment are attenuated. This amplified electrical response and attenuated optical response indicate that ABTS is engaged in oxidative redox-cycling, consistent with the electrochemical-generation of the $ABTS^{+\bullet}$-radical and its subsequent quenching by the melanin.

When the imposed potential was cycled into the reducing regions, peaks in reducing-current (shown as negative peaks)

and absorbance were also observed, indicating that the electrode could generate and quench the $PQ^{+\bullet}$-radical. Comparing with the control chitosan film, the melanin-containing films exhibit amplified reducing currents and attenuated absorbance, indicating that both melanins can quench the $PQ^{+\bullet}$-radical. It is important to note that detailed quantitative analysis of these results is constrained. (i) We could not precisely control the quantities of melanin in the films, preventing direct comparison of the responses between *Sepia* and fungal DHN melanins; (ii) the reducing potentials required for PQ^{2+}-reduction result in water reduction reactions, causing the reductive currents to encompass contributions from these interfering reactions. Despite these constraints, these studies demonstrate that melanin can quench radicals either by donating electrons to oxidative radicals or accepting electrons from reductive radicals.

To directly compare redox and radical scavenging activities, we prepared films containing four levels of fungal DHN melanin and probed with a cyclic imposed potential in the presence of Ru^{3+} (reductive mediator) and ABTS (oxidative mediator). To obtain a semi-quantitative estimate of redox capacity, as illustrated in Fig. 2e, we calculated the number of electrons (N_e) transferred to the DHN melanin during an oxidative segment by integrating the current to determine the charge transfer (Q), subtracting the Q observed for the control (melanin-free film, chitosan; Q_{Chit}), and converting these electrical measures into molar units using Faraday's constant. To quantify $ABTS^{+\bullet}$-radical scavenging activity, we calculated the fractional attenuation of optical absorbance in the oxidative segment (in this experiment, we measured absorbance at λ_{max} = 420 nm for the $ABTS^{+\bullet}$-radical). Fig. 2e shows a linear relationship between DHN melanin's radical-scavenging and redox-activities. In related experiments with PQ, we also observed a linear correlation between DHN melanin's redox capacity (*i.e.*, ability to accept electrons as measured electrically) and its $PQ^{+\bullet}$-radical scavenging activities as measured spectrally.[46]

In summary, these results are consistent with those from pulse radiolysis studies[39,40] and demonstrate that electrochemistry provides a simple and reagentless means to controllably generate free radicals, while spectral measurements enable the detection of radical generation and scavenging. Consistent with the redox activities observed in Fig. 1, multi-cycle studies (not shown) demonstrate that melanins can repeatedly quench free radicals by either donating electrons to oxidative radicals (*e.g.*, to $ABTS^{+\bullet}$) or accepting electrons from a reductive radical (*e.g.*, from $PQ^{+\bullet}$).[46] Following studies (not shown) also indicated that melanin's radical-scavenging activities depend on its redox-state: reduced (but not oxidized) melanin can effectively donate electrons to quench the $ABTS^{+\bullet}$-radical, while oxidized (but not reduced) melanin can effectively quench the $PQ^{+\bullet}$-radical.[46]

Electrochemical "poising" of redox-state

In the above sections, we focused on studies in which cyclic potential inputs were imposed and electrical and spectral output responses were measured to characterize melanin's redox-related properties. However, mediated electrochemistry is more flexible as it can be used to poise melanin's redox state to allow observation of redox-state-dependent responses. This is illustrated by studies to understand how *Sepia* melanin's ability to generate reactive oxygen species (ROS) depends on its redox state.

In these experiments,[52] we used indium-tin-oxide (ITO) coated glass electrodes and prepared chitosan-coated electrodes with varying amounts of *Sepia* melanin. The negative control film was a chitosan film without any redox-active components, while several positive control films were prepared by modifying chitosan films with catechol moieties (catechol-modified chitosan films are relatively well-studied example of redox-active and non-conducting film).[50,61,66,67] These film-coated electrodes were immersed in a mixture of Ru^{3+} (reductive mediator) and Fc (oxidative mediator). To poise the films in a reduced state, a reducing potential was imposed (−0.4 V *vs.* Ag/AgCl) for 5 min to enable Ru^{3+} to undergo reductive redox-cycling to transfer electrons from the electrode to the melanin. To estimate redox capacity of these reduced films, we then switched the electrode potential to an oxidative voltage (+0.7 V *vs.* Ag/AgCl) and measured the oxidative charge transferred (Q) over 5 min as illustrated in Fig. 3a (note the short times used for reduction and oxidation are insufficient to determine a true redox capacity). In this case, the redox capacity was estimated by subtracting the charge for the negative control from that of the sample film and the difference was converted into molar units using the Faraday constant. As expected, Fig. 3b shows that the redox capacity of the film increases with the melanin-content and was less than the capacity of a catechol–chitosan film (positive control).

In the next experiment,[52] we examined how melanin's redox state affects its ability to generate reactive oxygen species (*i.e.*, H_2O_2). For this study, we first poised the melanin-containing film in either a reduced or oxidized state (by imposing an appropriate electrode potential for 5 min) and then incubated these films in an air-saturated aqueous solution for 15 min. After incubation, we measured the H_2O_2 levels in the solution. Fig. 3c shows that the reduced melanin-containing films could generate H_2O_2 in proportion to the amount of melanin in the film, while the oxidized films showed little H_2O_2-generation. Fig. 3d shows that if the data is normalized in terms of the film's redox capacity, the melanin-containing films show the same relationship between H_2O_2-generation and the film's redox activity as measured by its capacity, N_e.

In summary, these studies[52] demonstrate that melanin can donate electrons to O_2 to generate ROS, but these ROS-generating pro-oxidant activities depend on melanin's redox-state. The obvious question from a biological function perspective is whether there are relevant contexts in which melanin can be poised in a reduced state yet be in the presence of O_2? We believe such contexts occur in metabolically-active environments that yield steep gradients in O_2 (*e.g.*, the lung, gut, and brain, and the soil rhizosphere).[68–72] In these biological contexts, the distance separating O_2-rich oxidative

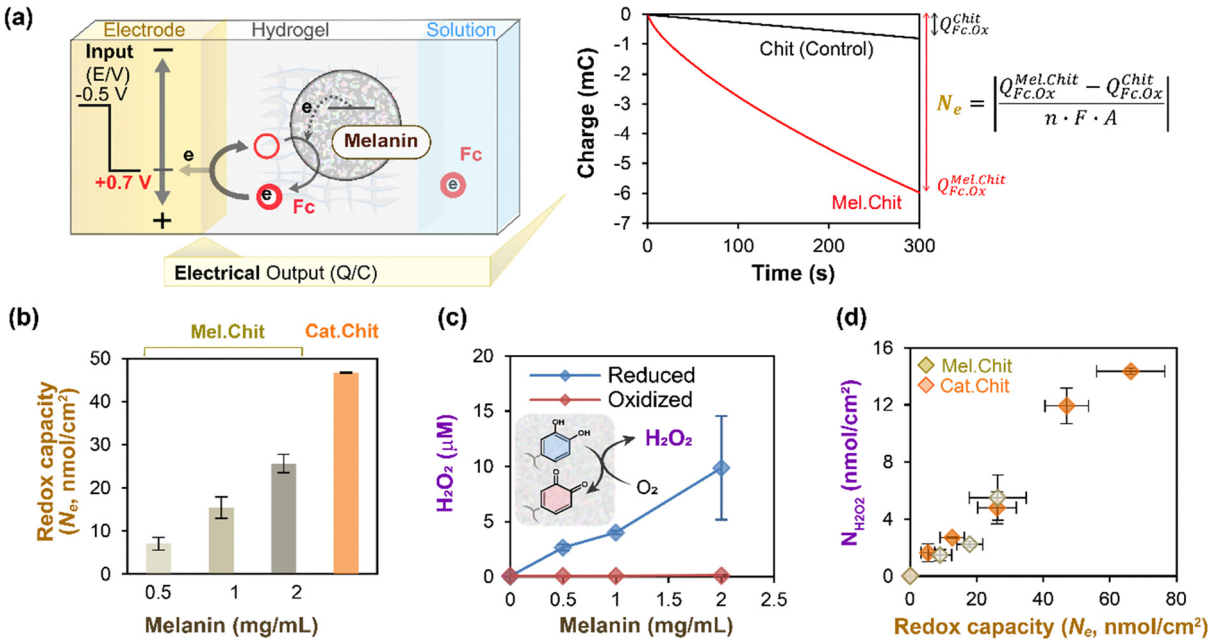

Fig. 3 Melanin can be electrochemically-poised in an oxidative or reductive state to allow study of its context-dependent ROS-generating activities. (a) Illustration of experimental and calculational approach. (b) As expected, films with greater levels of melanin have higher redox activities (*i.e.*, redox capacities). (c) Reduced (but not oxidized) melanin can donate electrons to O_2 to generate ROS (*i.e.*, H_2O_2). (d) Semi-quantitative relationship between melanin's ROS-generating and redox activities. Note: catechol–chitosan films serve as a positive control. [Adapted with permission from ref. 52. Copyright 2014, American Society, Washington, DC.].

conditions and O_2-depleted reductive conditions can be small (10–100 microns).

In most melanized tissues (*e.g.*, skin, eyes and brain), melanins are compartmentalized within organelles and possibly even conjugated to proteins,[73] and thus these natural melanins likely exist in forms that differ substantially from the melanin models commonly analyzed in the laboratory.[74] When this compartmentalization is disrupted by aging, pathological processes (*e.g.*, Parkinson's disease), or photoexposure (*e.g.*, in the retinal epithelium),[75,76] the melanins may be exposed to the O_2-rich oxidative conditions that permit ROS-generation (*e.g.*, H_2O_2). Importantly, melanins can also chelate metal ions, and iron accumulation in the substantia nigra has been invoked as one of the processes responsible for neuron loss in Parkinson's disease.[77,78] In the context of the oxidative conditions to which released melanin pigments may be exposed, the concomitant presence of iron and H_2O_2 could give rise to Fenton-type processes leading ultimately to generation of the highly reactive hydroxyl radicals. In contrast, melanins have also been reported to scavenge OH radicals.[15] So once again, it seems the context could determine the action of melanins – either a ROS-generator or ROS-scavenger.

Operando analysis

As noted above, spectroelectrochemical analysis sometimes allows the simultaneous observation of: (i) the electrical currents associated with mediated "flow" of electrons; and (ii) the spectral changes associated with redox-state switching of the participating molecules (*e.g.*, we showed this for the PQ^{2+} and ABTS "mediators" in Fig. 2). Unrelated studies with catechol-containing films showed that the film's spectral properties also change when its redox-state is switched.[57,59,79] Thus, we next measured spectral properties of melanin-containing films to determine if spectral changes could be detected when the melanin was being probed by mediators.[80] The experimental approach of observing spectral changes (associated with molecular changes in redox-state) at the same time that electrons are "passing through" the material (while the material is in operation) is referred to as operando analysis.

Two things enabled MEP analysis of melanin to be extended to operando analysis.[80] First, a soluble melanin from the black soldier fly (BSF) became available.[81] Unlike typical melanosome-derived melanin, the BSF melanin appears to be generated during insect sclerotization processes involving the oxidative coupling of dopamine derivatives.[82–85] When this soluble BSF-melanin was added to a chitosan film it was observed to spontaneously conjugate to the film (presumably through quinone-amine chemistries) to yield a semi-transparent BSF-melanin-chitosan film. Second, Fig. 4a shows a BSF-melanin film could be assembled on a transparent gold-electrode to allow spectral monitoring of the film during MEP. Experimentally, Fig. 4b shows MEP was performed using Ru^{3+} (reductive mediator) and Fc (oxidative mediator), and the film's absorbance was measured at 570 nm (the wavelength that showed the largest difference between oxidative and reductive segments of the cyclic voltammogram). This schematic also hypothesizes that melanin's redox-state switching involves catechol/quinone moieties.

Fig. 4c shows time series input-output curves for this BSF-melanin film when probed using a cyclic imposed potential in the presence of the Ru^{3+} and Fc mediators. The first electrical output, current (i), shows oscillations that are amplified for the melanin-chitosan film (*vs.* the control chitosan film). The second electrical output, charge transferred ($Q = \int i dt$), represents the total number of electrons transferred to/from the film during the oscillating input potentials. The oscillating Q is also amplified for the melanin-chitosan film. The spectral output, absorbance at 570 nm (Abs_{570}), is also observed to oscillate for the melanin-chitosan film while small oscillations are detected for the control chitosan film. This oscillating absorbance is consistent with the redox-state switching of the BSF-melanin during mediator probing. The vertical lines in Fig. 4c illustrate that the oscillations in Q and Abs_{570} are in-phase consistent with the conclusion that the electrons that flow into/from the film (measured by changes in Q) act to switch the redox-state of the film's BSF-melanin (measured by changes in Abs_{570}).

Consistent with the link between electron flow into/from the film and the film's redox-state switching, Fig. 4d[86,87] shows similar shapes for the Q–E and Abs_{570}–E phase-plane plots. The arrows in these plots indicate that under reducing potentials, electrons flow into the BSF-melanin film and switch the oxidized moieties (putative quinones) into reduced moieties

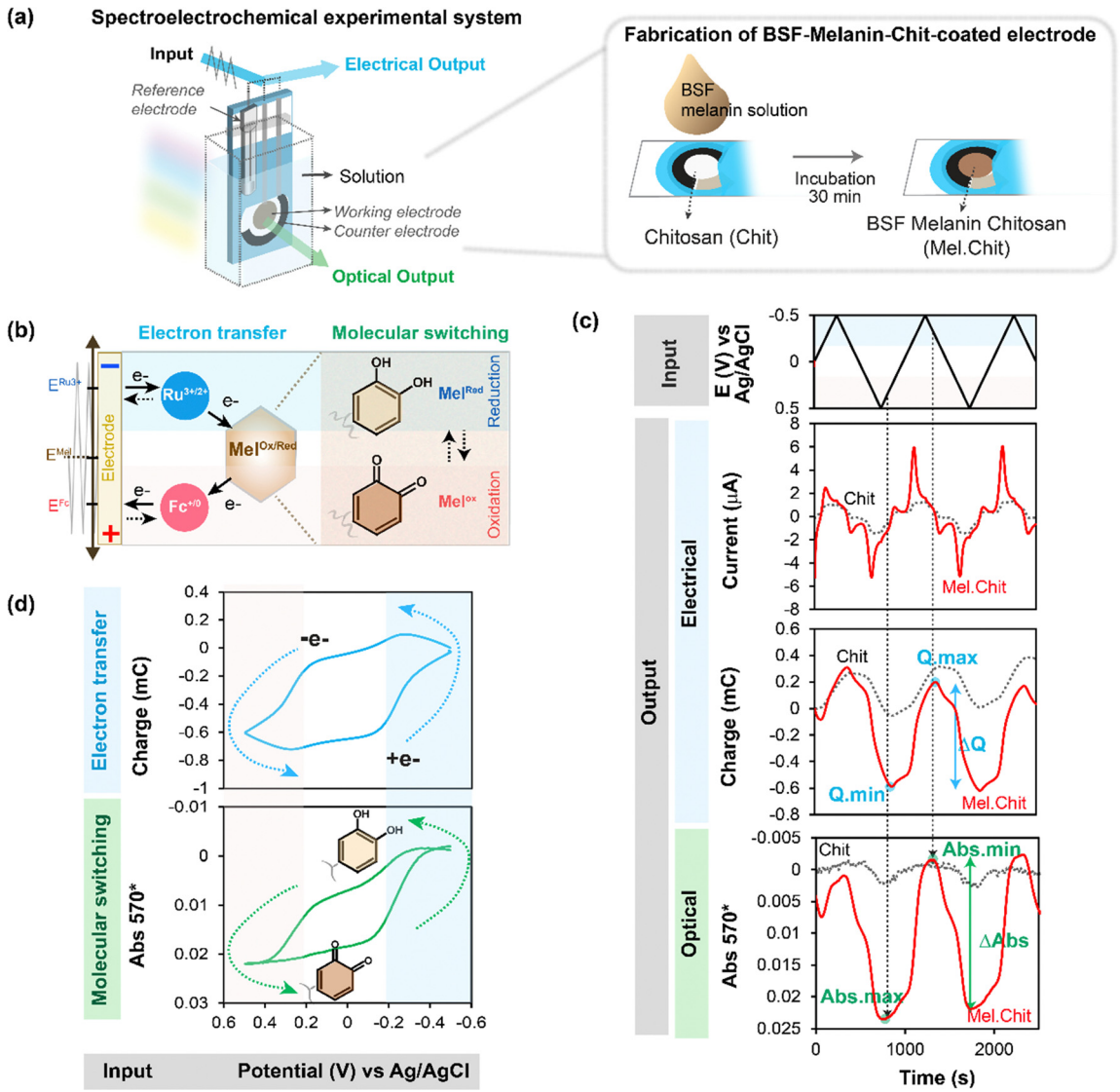

Fig. 4 Spectroelectrochemical operando analysis. (a) Melanin generated from the black soldier fly (BSF) is soluble and allows the fabrication of transparent melanin-chitosan films. (b) A transparent gold electrode allows spectroelectrochemical analysis of a partially-transparent hydrogel film of BSF melanin. (c) Time-series input-output curves for the melanin-chitosan film show that the amplified oscillating electrical charge (Q) and spectral output (Abs_{570}) are in-phase. (d) The similarity of the Q–E and Abs_{570}–E phase-plane plots indicates that as mediators are transferring electrons to/from melanin, the melanin is undergoing a simultaneous change in redox-state. Note: a chitosan film serves as a negative (redox-inactive) control. [Adapted with permission from ref. 80. Copyright 2023, American Society, Washington, DC.].

(putative catechols). Under oxidizing potentials, the arrows indicate that electrons are "flowing" from the film's BSF-melanin which is being switched from its reduced to its oxidized state.

In summary, these operando studies demonstrate that electron transfer to/from melanin involves its redox-state switching.

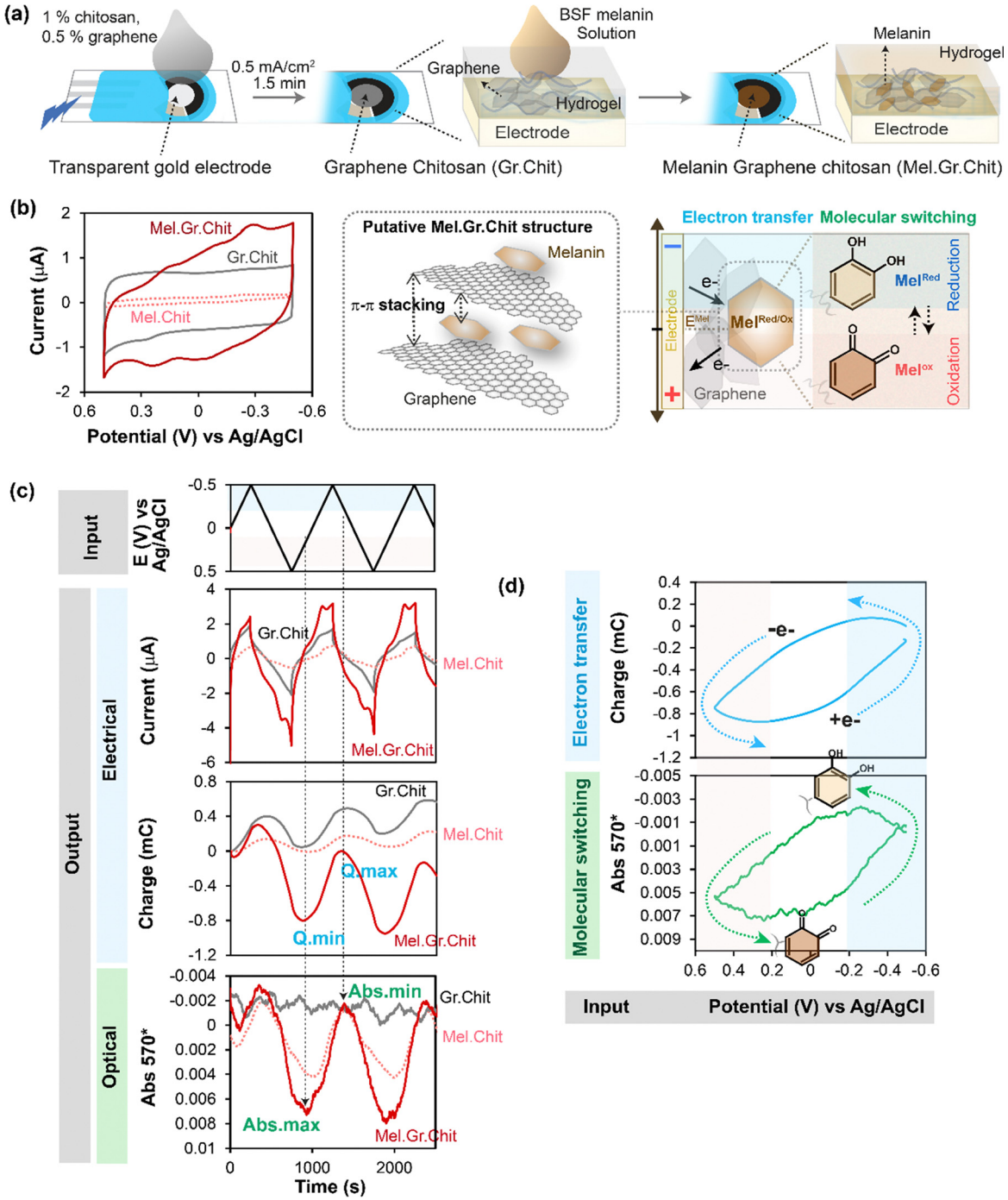

Fig. 5 Electrofabricated composite films of melanin–graphene–chitosan show direct electron transfer between graphene and BSF-melanin. (a) Schematic of the electrofabrication of the composite hydrogel films. (b) CVs (*i*–*E*; phase-plane plots) indicate that melanin–graphene–chitosan films have conducting properties (conferred by graphene) and redox activities (conferred by BSF-melanin). (c) Time-series input-output curves show cyclically-imposed electrical inputs (*i.e.*, potential) induce oscillating electrical outputs (*i* and *Q*) and spectral output (Abs_{570}) responses. (d) The similarity of the *Q*–*E* and Abs_{570}–*E* phase-plane plots indicates that melanin's redox state changes occur at the same time as the direct electron transfers *via* graphene (*i.e.*, no mediators were used in this study). Note: graphene-chitosan and melanin-chitosan films served as controls. [Adapted with permission from ref. 80. Copyright 2023, American Society, Washington, DC.].

Electrofabricated composite to detect direct electron transfer

A mentioned, we probe melanins that have been entrapped within a hydrogel film of the aminopolysaccharide chitosan. Chitosan was chosen because it possesses pH-responsive self-assembling properties that enable it to be easily electrodeposited as a hydrogel film on an electrode surface.[88–90] Importantly, components that can be blended into the chitosan deposition-solution can also be co-deposited and entrapped within the chitosan film. As illustrated in Fig. 5a, we co-deposited a graphene-chitosan film that offers conducting properties,[86,87] and then contacted this film-coated electrode with the black soldier fly (BSF) melanin to generate a melanin-graphene-chitosan composite film that has both conducting and redox active properties.

In initial electrochemical analysis,[80] we performed cyclic voltammetry (CV) and Fig. 5b shows the *i*–*E* phase-plane plot. The CV for the control melanin-chitosan film (Mel.Chit) shows small currents which indicates that while the BSF-melanin may confer redox-activity it is non-conductive (note: no mediators were used in these studies). The CV for the control graphene-chitosan film (Gr.Chit) shows a rectangular CV which is consistent with graphene conferring conducting properties to the film. The CV for the melanin-graphene-chitosan film (Mel.Gr.Chit) shows a rectangular shape that is complemented by broad peaks which suggest redox-based oxidation and reduction reactions.

Time series input-output curves are shown in Fig. 5c. When oscillating potential inputs were imposed, oscillating responses were observed in the current (*i*) and charge (*Q*), and the melanin-graphene-chitosan film showed amplifications in these electrical outputs (compared to either the graphene-chitosan control or the melanin-chitosan control). The spectral output response (Abs_{570}) for the melanin-graphene-chitosan film was also observed to oscillate consistent with a redox-state switching of the melanin. As observed in Fig. 4c, the vertical lines in the time series outputs in Fig. 5c show the electrical charge response (*Q*) is in-phase with the spectral response (Abs_{570}). Also similar to Fig. 4d and 5d shows the *Q*–*E* and Abs_{570}–*E* phase-plane plots have similar shapes consistent with the explanation that the direct transfer of electrons through the graphene to the melanin results in a redox-state-switching of the melanin.

In summary, these results indicate that BSF-melanin can directly exchange electrons with graphene and this exchange results in a switching of melanin's redox state. Potentially this extrinsic electron exchange involves π–π interactions between the graphene and melanin.[6,8,12,91,92] We should note that our analysis indicates that only a fraction of the redox-active BSF melanin moieties added to the film could undergo direct electron exchange, while the remaining BSF melanin moieties could only exchange electrons if diffusible mediators were provided.

Perspectives

Melanin is reported to offer important biological and technological properties that include: antimicrobial,[93,94] antioxidant[95,96] and anti-cancer activities;[97,98] radiation protective[99,100] and photothermal energy conversion properties;[101] and heavy metal binding abilities.[102,103] Because of melanin's structural complexity, it has been difficult to apply conventional bottom-up molecular-structure-based approaches to understand these various properties. As a result of this challenge, various top-down methods are being used to characterize melanin's functional properties.

We are developing electrochemical methods to characterize melanin's redox activities. Mediated electrochemical probing (MEP) has shown that melanins from various sources: are reversibly redox-active; have redox potentials in the mid-physiological range; and can accept electrons from a broad range of reductants and donate electrons to a broad range of oxidants. Spectroelectrochemical measurements enabled us to show that melanin can accept electrons to quench reductive free radicals or donate electrons to quench oxidative radicals. Spectroelectrochemical operando analysis showed that melanins can exchange electrons directly or indirectly (*i.e.*, *via* mediators), and during electron transfer melanin's redox-state is switched.

The recognition that melanin can exist in different redox states helps to explain how melanin's properties can depend on context. Specifically, depending on its redox-state, melanin can serve as either a reductant or an oxidant. However, context also depends on the environment. For instance, melanin's ability to donate electrons could perform an antioxidant function if electron-donation quenches an oxidative radical, or alternatively could perform a pro-oxidant function if electron-donation to O_2 generates reactive oxygen species (ROS). In fact, melanins can be viewed as redox-catalysts that promote the transfer of electrons from reductants to oxidants. Such catalytic properties may promote redox-cycling especially if melanin is localized within an O_2-gradient in which aerobic and anaerobic environments are separated by short diffusion distances (*i.e.*, tens of microns). We believe our observation that melanin can undergo redox-cycling with environmental chemicals and drugs may provide new and important insights of chemical toxicities and off-target drug activities.

The fabrication of composite films with graphene and black-soldier-fly (BSF) melanin and the operando analysis of these films enabled us to show that electrons can be directly transferred from an electrode through graphene to switch melanin's redox state. Potentially, this direct electron transfer may involve interactions between graphene and melanin's π-electrons as suggested in Fig. 5b. Future studies may assist in understanding how melanin's redox activities are related to its reported electronic and ionic conductivities.[7,20,22,74,104–107]

With an even greater level of speculation, one can ponder whether melanins play an energetic role in biology. In technology, redox-active catechols are gaining increasing attention as supercapacitors because they offer redox-capacitance for increased energy storage.[21,42,108–111] Since melanins also accept, store and donate electrons, they also offer redox capacitor properties, and the question is whether biology utilizes this energy-storage capability? The pigmented epithelium of the retina of migratory birds has long prolongations filled with melanin[112] which might serve as light/energy capacitor during nocturnal flights.[113] Tantalizing

evidence suggests that melanin may enable fungi to harvest radiation energy through yet-to-be discovered metabolic mechanisms.[114,115] Melanin-mediated ionizing radiation-sensing in radio-adapted strains of melanized fungi resulted in their enhanced growth in comparison with non-melanized controls and provided more resistance to environmental oxidants such as H_2O_2.[116,117] Currently it is not known if/how biology uses melanin for energy harvesting and storage and if it does, whether redox mechanisms are involved. However, this example illustrates that there remain many unanswered questions concerning melanin's biological function.

Conflicts of interest

There are no conflicts to declare.

Acknowledgements

This work was supported by the National Science Foundation (CBET #1932963 and MCB #2227598), the Defense Threat Reduction Agency (HDTRA1-19-0021), and the Gordon and Betty Moore Foundation (#11395).

References

1 M. d'Ischia, A. Napolitano, A. Pezzella, P. Meredith and M. Buehler, *Angew. Chem., Int. Ed.*, 2020, **59**, 11196–11205.
2 W. Cao, X. Zhou, N. C. McCallum, Z. Hu, Q. Z. Ni, U. Kapoor, C. M. Heil, K. S. Cay, T. Zand, A. J. Mantanona, A. Jayaraman, A. Dhinojwala, D. D. Deheyn, M. D. Shawkey, M. D. Burkart, J. D. Rinehart and N. C. Gianneschi, *J. Am. Chem. Soc.*, 2021, **143**, 2622–2637.
3 W. Xie, E. Pakdel, Y. Liang, Y. Jo Kim, D. Liu, L. Sun and X. Wang, *Biomacromolecules*, 2019, **20**, 4312–4331.
4 J. D. Simon and D. N. Peles, *Acc. Chem. Res.*, 2010, **43**, 1452–1460.
5 I. E. Pralea, R. C. Moldovan, A. M. Petrache, M. Ilieş, S. C. Hegheş, I. Ielciu, R. Nicoară, M. Moldovan, M. Ene, M. Radu, A. Uifălean and C. A. Iuga, *Int. J. Mol. Sci.*, 2019, **20**, 3943.
6 A. Thompson, F. E. Robles, J. W. Wilson, S. Deb, R. Calderbank and W. S. Warren, *Sci. Rep.*, 2016, **6**, 36871.
7 A. A. R. Watt, J. P. Bothma and P. Meredith, *Soft Matter*, 2009, **5**, 3754–3760.
8 C. Grieco, F. R. Kohl, A. T. Hanes and B. Kohler, *Nat. Commun.*, 2020, **11**, 1–9.
9 K. Y. Ju, M. C. Fischer and W. S. Warren, *ACS Nano*, 2018, **12**, 12050–12061.
10 M. L. Tran, B. J. Powell and P. Meredith, *Biophys. J.*, 2006, **90**, 743–752.
11 M. Xiao, M. D. Shawkey and A. Dhinojwala, *Adv. Opt. Mater.*, 2020, **8**, 2000932.
12 E. Vahidzadeh, A. P. Kalra and K. Shankar, *Biosens. Bioelectron.*, 2018, **122**, 127–139.
13 P. Manini, V. Lino, G. D'Errico, S. Reale, A. Napolitano, F. De Angelis and M. D'Ischia, *Polym. Chem.*, 2020, **11**, 5005–5010.
14 B.-L. L. Seagle, E. M. Gasyna, W. F. Mieler and J. R. Norris, *Proc. Natl. Acad. Sci. U. S. A.*, 2006, **103**, 16644–16648.
15 S. Jiang, X. M. Liu, X. Dai, Q. Zhou, T. C. Lei, F. Beermann, K. Wakamatsu and S. Z. Xu, *Free Radical Biol. Med.*, 2010, **48**, 1144–1151.
16 M. Brenner and V. J. Hearing, *Photochem. Photobiol.*, 2008, **84**, 539–549.
17 R. Micillo, L. Panzella, M. Iacomino, G. Prampolini, I. Cacelli, A. Ferretti, O. Crescenzi, K. Koike, A. Napolitano and M. D'Ischia, *Sci. Rep.*, 2017, **7**, 41532.
18 S. Premi, S. Wallisch, C. M. Mano, A. B. Weiner, A. Bacchiocchi, K. Wakamatsu, E. J. H. H. Bechara, R. Halaban, T. Douki and D. E. Brash, *Science*, 2015, **347**, 842.
19 M. Gauden, A. Pezzella, L. Panzella, A. Napolitano, M. D'Ischia and V. Sundstro, *J. Phys. Chem. B*, 2009, **113**, 12575–12580.
20 A. B. Mostert, B. J. Powell, F. L. Pratt, G. R. Hanson, T. Sarna, I. R. Gentle and P. Meredith, *Proc. Natl. Acad. Sci. U. S. A.*, 2012, **109**, 8943–8947.
21 M. Reali, A. Gouda, J. Bellemare, D. Ménard, J.-M. M. Nunzi, F. Soavi and C. Santato, *ACS Appl. Bio Mater.*, 2020, **3**, 5244–5252.
22 A. Bernardus Mostert, B. J. Powell, I. R. Gentle and P. Meredith, *Appl. Phys. Lett.*, 2012, **100**, 093701.
23 M. Sheliakina, A. B. Mostert and P. Meredith, *Adv. Funct. Mater.*, 2018, **28**, 1805514.
24 J. V. Paulin, A. P. Coleone, A. Batagin-Neto, G. Burwell, P. Meredith, C. F. O. Graeff and A. B. Mostert, *J. Mater. Chem. C*, 2021, **9**, 8345–8358.
25 J. McGinness, P. Corry and P. Proctor, *Science*, 1974, **183**, 853–855.
26 B. D. Paulsen, K. Tybrandt, E. Stavrinidou and J. Rivnay, *Nat. Mater.*, 2020, **19**, 13–26.
27 A. J. Nappi and B. M. Christensen, *Insect Biochem. Mol. Biol.*, 2005, **35**, 443–459.
28 B. M. Christensen, J. Li, C.-C. Chen and A. J. Nappi, *Trends Parasitol.*, 2005, **21**, 192–199.
29 E. S. Jacobson, *Clin. Microbiol. Rev.*, 2000, **13**, 708–717.
30 E. S. Jacobson and J. D. Hong, *J. Bacteriol.*, 1997, **179**, 5340–5346.
31 J. D. Nosanchuk and A. Casadevall, *Antimicrob. Agents Chemother.*, 2006, **50**, 3519–3528.
32 R. J. B. Cordero and A. Casadevall, *Fungal Biol. Rev.*, 2017, **31**, 99–112.
33 E. S. Jacobson, E. Hove and H. S. Emery, *Infect. Immun.*, 1995, **63**, 4944–4945.
34 H. Zhang, C. Huang, J. Zhang, C. Wang, T. Wang, S. Shi, Z. Gu and Y. Li, *Giant*, 2022, **12**, 100120.
35 L. Panzella, G. D'Errico, G. Vitiello, M. Perfetti, M. L. Alfieri, A. Napolitano and M. D'Ischia, *Chem. Commun.*, 2018, **54**, 9426–9429.
36 J. D. Simon, L. Hong and D. N. Peles, *J. Phys. Chem. B*, 2008, **112**, 13201–13217.

37 A. Napolitano, L. Panzella, G. Monfrecola and M. D'Ischia, *Pigm. Cell Melanoma Res.*, 2014, **27**, 721–733.
38 E. Obrador, F. Liu-Smith, R. W. Dellinger, R. Salvador, F. L. Meyskens and J. M. Estrela, *Biol. Chem.*, 2019, **400**, 589–612.
39 T. Sarna, B. Pilas, E. J. Land and T. G. Truscott, *Biochim. Biophys. Acta, Gen. Subj.*, 1986, **883**, 162–167.
40 M. Rózanowska, T. Sarna, E. J. Land and T. G. Truscott, *Free Radical Biol. Med.*, 1999, **26**, 518–525.
41 J. M. Menter and I. Willis, *Pigm. Cell Res.*, 1997, **10**, 214–217.
42 R. Xu, A. Gouda, M. F. Caso, F. Soavi and C. Santato, *ACS Omega*, 2019, **4**, 12244–12251.
43 R. Xu, F. Soavi and C. Santato, *Front. Bioeng. Biotechnol.*, 2019, **7**, 227.
44 S. Gidanian and P. J. Farmer, *J. Inorg. Biochem.*, 2002, **89**, 54–60.
45 M. Kang, E. Kim, Z. Temoçin, J. Li, E. Dadachova, Z. Wang, L. Panzella, A. Napolitano, W. E. W. E. Bentley and G. F. G. F. Payne, *Chem. Mater.*, 2018, **30**, 5814–5826.
46 E. Kim, M. Kang, T. Tschirhart, M. Malo, E. Dadachova, G. Cao, J. J. Yin, W. E. Bentley, Z. Wang and G. F. Payne, *Biomacromolecules*, 2017, **18**, 4084–4098.
47 Z. Temoçin, E. Kim, J. Li, L. Panzella, M. L. M. L. Alfieri, A. Napolitano, D. L. D. L. Kelly, W. E. W. E. Bentley and G. F. G. F. Payne, *ACS Chem. Neurosci.*, 2017, **8**, 2766–2777.
48 E. Kim, W. T. Leverage, Y. Liu, L. Panzella, M. L. Alfieri, A. Napolitano, W. E. Bentley and G. F. Payne, *ACS Chem. Neurosci.*, 2016, **7**, 1057–1067.
49 E. Kim, L. Panzella, R. Micillo, W. E. Bentley, A. Napolitano and G. F. Payne, *Sci. Rep.*, 2015, **5**, 18447.
50 E. Kim, Y. Liu, C. J. Baker, R. Owens, S. Xiao, W. E. Bentley and G. F. Payne, *Biomacromolecules*, 2011, **12**, 880–888.
51 E. Kim, L. Panzella, A. Napolitano and G. F. Payne, *J. Invest. Dermatol.*, 2020, **140**, 537–543.
52 E. Kim, Y. Liu, W. T. T. Leverage, J.-J. J.-J. J. Yin, I. M. I. M. White, W. E. W. E. Bentley and G. F. G. F. Payne, *Biomacromolecules*, 2014, **15**, 1653–1662.
53 E. Kim, T. Gordonov, Y. Liu, W. E. W. E. Bentley and G. F. G. F. Payne, *ACS Chem. Biol.*, 2013, **8**, 716–724.
54 S. Iijima, B. S. Sherigara, W. Kutner, F. Souza, Y.-P. Sun, A. Star, D. W. Steuerman, J. R. Heath and J. F. Stoddart, *Angew. Chem., Int. Ed. Engl*, 1991, **354**, 5045.
55 M. E. M. E. Lee, E. Kim, Y. Liu, J. C. J. C. March, W. E. W. E. Bentley and G. F. G. F. Payne, *J. Agric. Food Chem.*, 2014, **62**, 9760–9768.
56 S. Wu, E. Kim, J. Li, W. E. Bentley, X. W. Shi and G. F. Payne, *ACS Appl. Electron. Mater.*, 2019, **1**, 1337–1347.
57 Z. Zhao, S. Wu, E. Kim, C. Y. Chen, J. R. Rzasa, X. Shi, W. E. Bentley and G. F. Payne, *ACS Appl. Electron. Mater.*, 2022, **4**, 2490.
58 E. Kim, Z. Liu, Y. Liu, W. Bentley and G. Payne, *Biomimetics*, 2017, **2**, 11.
59 S. Wu, E. Kim, C. Y. Chen, J. Li, E. VanArsdale, C. Grieco, B. Kohler, W. E. Bentley, X. Shi and G. F. Payne, *Adv. Electron. Mater.*, 2020, **6**, 2000452.
60 E. Kim, Y. Xiong, Y. Cheng, H. C. Wu, Y. Liu, B. H. Morrow, H. Ben-Yoav, R. Ghodssi, G. W. Rubloff, J. Shen, W. E. Bentley, X. Shi and G. F. Payne, *Polymers*, 2015, **7**, 1–46.
61 E. Kim, Y. Liu, X. Shi, X. Yang, W. E. Bentley and P. F. Gregory, *Adv. Funct. Mater.*, 2010, **20**, 2683–2694.
62 H. Liu, X. Qu, E. Kim, M. Lei, K. Dai, X. Tan, M. Xu, J. Li, Y. Liu, X. Shi, P. Li, G. F. G. F. Payne and C. Liu, *Biomaterials*, 2018, **162**, 109–122.
63 Z. Wang, T. Tschirhart, Z. Schultzhaus, E. E. Kelly, A. Chen, E. Oh, O. Nag, E. R. Glaser, E. Kim, P. F. Lloyd, P. T. Charles, W. Li, D. Leary, J. Compton, D. A. Phillips, A. Dhinojwala, G. F. Payne and G. J. Vora, *Appl. Environ. Microbiol.*, 2020, **86**, e02749-19.
64 H. C. Eisenman and A. Casadevall, *Appl. Microbiol. Biotechnol.*, 2012, **93**, 931–940.
65 D. M. Dixon, P. J. Szaniszlo and A. Polak, in *The fungal spore and disease initiation in plants and animals*, ed. G. T. Cole and H. C. Hoch, Plenum Press, New York, 1991.
66 C. Cao, E. Kim, Y. Liu, M. Kang, J. Li, J. J. Yin, H. Liu, X. Qu, C. Liu, W. E. W. E. Bentley and G. F. G. F. Payne, *Biomacromolecules*, 2018, **19**, 3502–3514.
67 E. Kim, Y. Liu, W. E. W. E. Bentley and G. F. G. F. Payne, *Adv. Funct. Mater.*, 2012, **22**, 1409–1416.
68 R. K. Fritts, A. L. McCully and J. B. McKinlay, *Microbiol. Mol. Biol. Rev.*, 2021, **85**, e00135-20.
69 J. Li, Z. Zhao, E. Kim, J. R. Rzasa, G. Zong, L.-X. Wang, W. E. Bentley and G. F. Payne, *iScience*, 2022, **25**, 104548.
70 A. W. Fuller, P. Young, B. D. Pierce, J. Kitson-Finuff, P. Jain, K. Schneider, S. Lazar, O. Taran, A. G. Palmer and D. G. Lynn, *PLoS One*, 2017, **12**, 0182655.
71 O. Taran, V. Patel and D. G. Lynn, *Chem. Commun.*, 2019, **55**, 3602–3605.
72 S. Liu, Y. H. Lin, A. Murphy, J. Anderson, N. Walker, D. G. Lynn, A. N. Binns and B. D. Pierce, *Front. Plant Sci.*, 2020, **11**, 1074.
73 E. Monzani, S. Nicolis, S. Dell'Acqua, A. Capucciati, C. Bacchella, F. A. Zucca, E. V. Mosharov, D. Sulzer, L. Zecca and L. Casella, *Angew. Chem., Int. Ed.*, 2019, **131**, 6580–6596.
74 L. Panzella, G. Gentile, G. Derrico, N. F. Della Vecchia, M. E. Errico, A. Napolitano, C. Carfagna, M. Dischia, G. Gentile, M. E. Errico, C. Carfagna, G. D'Errico, N. F. Della Vecchia, M. E. Errico, A. Napolitano, C. Carfagna and M. D'Ischia, *Angew. Chem., Int. Ed.*, 2013, **52**, 12684–12687.
75 S. Ito, A. Pilat, W. Gerwat, C. M. B. Skumatz, M. Ito, A. Kiyono, A. Zadlo, Y. Nakanishi, L. Kolbe, J. M. Burke, T. Sarna and K. Wakamatsu, *Pigm. Cell Melanoma Res.*, 2013, **26**, 357–366.
76 A. Żądło, S. Ito, M. Sarna, K. Wakamatsu, K. Mokrzyński and T. Sarna, *Photochem. Photobiol. Sci.*, 2020, **19**, 654–667.
77 M. Gerlach, K. L. Double, D. Ben-Shachar, L. Zecca, M. B. H. Youdim and P. Riederer, *Neurotoxic. Res.*, 2003, **5**, 35–43.
78 L. Zecca, A. Stroppolo, A. Gatti, D. Tampellini, M. Toscani, M. Gallorini, G. Giaveri, P. Arosio, P. Santambrogio,

R. G. Fariello, E. Karatekin, M. H. Kleinman, N. Turro, O. Hornykiewicz and F. A. Zucca, *Proc. Natl. Acad. Sci. U. S. A.*, 2004, **101**, 9843–9848.

79 S. Wu, Z. Zhao, J. R. Rzasa, E. Kim, J. Li, E. VanArsdale, W. E. Bentley, X. Shi and G. F. Payne, *Adv. Funct. Mater.*, 2021, **31**, 2007709.

80 E. Kim, C. Chen, J. Wei Phua, A. Napolitano, W. E. Bentley and G. F. Payne, *J. Phys. Chem. C*, 2023, **127**, 19979–19994.

81 U. D'Amora, A. Soriente, A. Ronca, S. Scialla, M. Perrella, P. Manini, J. W. Phua, C. Ottenheim, R. Di Girolamo, A. Pezzella, M. G. Raucci and L. Ambrosio, *Biomedicines*, 2022, **10**, 2945.

82 Y. Arakane, M. Y. Noh, T. Asano and K. J. Kramer, *Extracellular Composite Matrices in Arthropods*, Springer International Publishing, Cham, 2016, pp. 165–220.

83 M. Sugumaran, *Pigm. Cell Res.*, 2002, **15**, 2–9.

84 S. O. Andersen, *Insect Biochem. Mol. Biol.*, 2010, **40**, 166–178.

85 H. K. Ravi, A. Degrou, J. Costil, C. Trespeuch, F. Chemat and M. A. Vian, *Processes*, 2020, **8**, 857.

86 E. Kim, R. Argenziano, Z. Zhao, C. Y. Chen, M. Shen, W. E. Bentley, A. Napolitano and G. F. Payne, *Adv. Mater. Interfaces*, 2022, **9**, 2202021.

87 M. Kang, E. Kim, T. E. T. E. Winkler, G. Banis, Y. Liu, C. A. C. A. Kitchen, D. L. D. L. Kelly, R. Ghodssi and G. F. G. F. Payne, *Biosens. Bioelectron.*, 2017, **95**, 55–59.

88 J. Li, S. S. Wu, E. Kim, K. Yan, H. Liu, C. Liu, H. Dong, X. Qu, X. Shi, J. Shen, W. E. W. E. Bentley and G. F. G. F. Payne, *Biofabrication*, 2019, **11**, 032002.

89 S. Wu, K. Yan, J. Li, R. N. Huynh, C. B. Raub, J. Shen, X. Shi and G. F. Payne, *React. Funct. Polym.*, 2020, **148**, 104492.

90 Y. Cheng, X. Luo, J. Betz, S. Buckhout-White, O. Bekdash, G. F. Payne, W. E. Bentley and G. W. Rubloff, *Soft Matter*, 2010, **6**, 3177–3183.

91 C. Bonavolontà, C. De Lisio, M. D'Ischia, P. Maddalena, P. Manini, A. Pezzella and M. Valentino, *Sci. Rep.*, 2017, **7**, 1–8.

92 F. R. Kohl, C. Grieco and B. Kohler, *Chem. Sci.*, 2020, **11**, 1248–1259.

93 I. Ben Tahar, M. Kus-Liśkiewicz, Y. Lara, E. Javaux and P. Fickers, *Biotechnol. Prog.*, 2020, **36**, e2912.

94 T. Rahmani Eliato, J. T. Smith, Z. Tian, E. S. Kim, W. Hwang, C. P. Andam and Y. J. Kim, *J. Mater. Chem. B*, 2021, **9**, 1536–1545.

95 P. Manini, M. Bietti, M. Galeotti, M. Salamone, O. Lanzalunga, M. M. Cecchini, S. Reale, O. Crescenzi, A. Napolitano, F. De Angelis, V. Barone and M. D'Ischia, *ACS Omega*, 2018, **3**, 3918–3927.

96 L. Panzella, L. Leone, G. Greco, G. Vitiello, G. D'Errico, A. Napolitano and M. d'Ischia, *Pigm. Cell Melanoma Res.*, 2014, **27**, 244–252.

97 O. Al-Obeed, A. S. El-Obeid, S. Matou-Nasri, M. A. Vaali-Mohammed, Y. Alhaidan, M. Elwatidy, H. Al Dosary, Z. Alehaideb, K. Alkhayal, A. Haseeb, J. McKerrow, R. Ahmad and M. H. Abdulla, *Cancer Cell Int.*, 2020, **20**, 1–17.

98 N. E. A. El-Naggar and S. M. El-Ewasy, *Sci. Rep.*, 2017, **7**, 1–19.

99 L. Guo, W. Li, Z. Gu, L. Wang, L. Guo, S. Ma, C. Li, J. Sun, B. Han and J. Chang, *Int. J. Mol. Sci.*, 2023, **24**, 4360.

100 W. Song, H. Yang, S. Liu, H. Yu, D. Li, P. Li and R. Xing, *J. Mater. Chem. B*, 2023, **11**, 7528–7543.

101 H. Liu, Y. Yang, Y. Liu, J. Pan, J. Wang, F. Man, W. Zhang and G. Liu, *Adv. Sci.*, 2020, **7**, 1903129.

102 A. S. ElObeid, A. Kamal-Eldin, M. A. K. Abdelhalim and A. M. Haseeb, *Basic Clin. Pharmacol. Toxicol.*, 2017, **120**, 515–522.

103 V. Manirethan, N. Gupta, R. M. Balakrishnan and K. Raval, *Environ. Sci. Pollut. Res.*, 2020, **27**, 24723–24737.

104 T. Sarna and P. M. Plonka, in *Biomedical EPR, Part A: Free Radicals, Metals, Medicine, and Physiology*, ed. S. R. Eaton, G. R. Eaton and L. J. Berliner, Springer US, Boston, MA, 2005, pp. 125–146.

105 Y. J. Kim, W. Wu, S.-E. Chun, J. F. Whitacre and C. J. Bettinger, *Adv. Mater.*, 2014, **26**, 6572–6579.

106 Y. J. Kim, A. Khetan, W. Wu, S. E. Chun, V. Viswanathan, J. F. Whitacre and C. J. Bettinger, *Adv. Mater.*, 2016, **28**, 3173–3180.

107 Z. Tian, W. Hwang and Y. J. Kim, *J. Mater. Chem. B*, 2019, **7**, 6355–6361.

108 L. Yang, X. Guo, Z. Jin, W. Guo, G. Duan, X. Liu and Y. Li, *Nano Today*, 2021, **37**, 101075.

109 A. Camus, M. Reali, M. Rozel, M. Zhuldybina, F. Soavi and C. Santato, *Proc. Natl. Acad. Sci. U. S. A.*, 2022, **119**, e2200058119.

110 C. A. Milroy and A. Manthiram, *ACS Energy Lett.*, 2016, **1**, 672–677.

111 A. S. Sharova, F. Melloni, G. Lanzani, C. J. Bettinger and M. Caironi, *Adv. Mater. Technol.*, 2021, **6**, 2000757.

112 N. F. Bassuoni, M. M. A. Abumandour, A. El-Mansi and B. G. Hanafy, *Microsc. Res. Tech.*, 2022, **85**, 607–616.

113 G. Goodman and D. Bercovich, *Med. Hypotheses*, 2008, **71**, 190–202.

114 E. Dadachova and A. Casadevall, *Curr. Opin. Microbiol.*, 2008, **11**, 525–531.

115 E. Dadachova, R. A. Bryan, X. Huang, T. Moadel, A. D. Schweitzer, P. Aisen, J. D. Nosanchuk and A. Casadevall, *PLoS One*, 2007, **2**, e457.

116 M. E. Malo, C. Frank and E. Dadachova, *Fungal Biol.*, 2020, **124**, 368–375.

117 M. E. Malo, Z. Schultzhaus, C. Frank, J. Romsdahl, Z. Wang and E. Dadachova, *Comput. Struct. Biotechnol. J.*, 2021, **19**, 196–205.